Chapter 2

Literature review and the state-of-the-art

This chapter provides a comprehensive review on land surface measurements, rough surface scattering theories, volume scattering theories, and scatterometers supplemented with the literature on experimental data to validate the applicability domains of the presented approaches. In addition to the literature review, the state-of-the-art knowledge has also been presented in this chapter.

2.1 The role of scattering model

The geometry of most of the Earth's topography is formed by the superposition of two factors: a quasi-deterministic shape and its random fluctuation. The soil surface has a mean border to which random height variations are added. However, a vegetation canopy has been approximated as scatterers of varying shapes, sizes, and orientations, defined by probability distributions. Similar statements can be made about various types of terrain. The probabilistic character of terrain targets and the peculiarities of their shape and direction make modeling bistatic scattering a demanding challenge. Using the scattering

model, we can anticipate how the radar scattering coefficient would behave in relation to a specific terrain parameter of interest and use it to explain experimental findings. So, in order to develop a scattering model, we should keep the following things in our mind:

✓Try to characterize the surface topographical and morphological features using statistical distributions, such as height, and inclination statistics for random surfaces, size and geometry distributions for volume scatterers, etc., and

✓Construct surfaces and volumes based on the approximations and compute the scattering cross-sections for each constructed target's radar wave parameter of interest; then do an ensemble average.

The scattering models are helpful for radar remote sensing and investigating terrain emissions observed by the radiometers. This can be done by integrating bistatic scattering coefficients' overall scattering directions.

2.2 A review of land observations and surface scattering model

2.2.1 Land parameters observation

In this section of the chapter, we've covered the basic terms related to the natural surface terrain's physical and statistical features. The roughness and smoothness of a surface are described by statistical parameters measured in wavelength units. There are four important parameters used to characterize the natural surface within the surface model.

✓**Root mean square (RMS) height (s)**

✓**Surface correlation length (l)**

✓**RMS slope (m)**

✓**Volumteric soil moisture (m_v)**

All three surface statistical parameters are connected with the random component of the surface height relative to the reference surface. The reference surface can be the deterministic periodic patterns, shown in Figure 2.1 (a), or a mean surface for a randomly oriented surface, as shown in Figure 2.1 (b). The explanation of the random non-periodic surface situation is detailed in this section

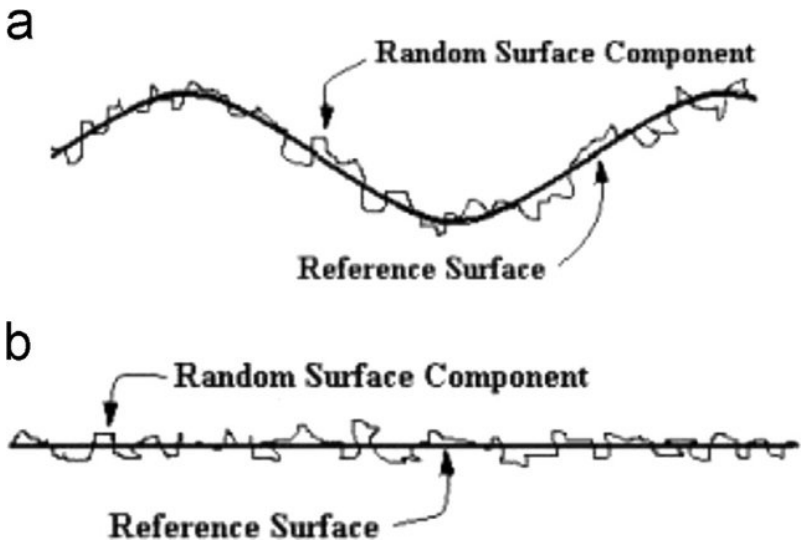

Fig. 2.1 (a) Random height variations superimposed on a periodic surface; and (b) Random height variations superimposed on a flat surface

Source:www.researchgate.net/publication/277339229_Fast_computation_of_bare_soil_surface_roughness_on_a_Fermi_GPU/figures?lo=1

✓RMS height

Typically, the Gaussian probability density function $p(z)$ is used to quantify the height $z(x,y)$ above the $x-y$ plane for a random surface whose mean coincides with the $x-y$ plane. The function $p(z)$ is given by the Equation 2.1:

$$p(z) = \frac{1}{\sqrt{2\pi s^2}} e^{\frac{-z^2}{2s^2}} \tag{2.1}$$

Where, s represents the RMS height.

$$s = < z^2 >^2 = [\int_{\infty}^{-\infty} z^2 p(z) dz]^{\frac{1}{2}} \tag{2.2}$$

Alternatively, the mean heights $\bar{z}$ and $\bar{z^2}$ can be determined from z of a statistically representative surface segment of dimensions L_x and L_y, centered at the origin, as shown in Equations 2.3 and 2.4.

$$\bar{z} = \frac{1}{L_x L_y} \int_{\frac{-L_x}{2}}^{\frac{L_x}{2}} \int_{\frac{-L_y}{2}}^{\frac{L_y}{2}} z(x,y) dx dy \tag{2.3}$$

$$\bar{z^2} = \frac{1}{L_x L_y} \int_{\frac{-L_x}{2}}^{\frac{L_x}{2}} \int_{\frac{-L_y}{2}}^{\frac{L_y}{2}} z^2(x,y) dx dy \tag{2.4}$$

The RMS height is then expressed as

$$s = (\bar{z^2} - \bar{z}^2)^{\frac{1}{2}} \tag{2.5}$$

For azimuthally symmetric surfaces, a one-dimensional height profile $z(x)$ is adequate and integration over y is not required. In practice, An adequate spacing (i.e., Δx) is used to digitize the profile in order to produce its discrete values of $z_i(x_i)$. No noticeable influence on reflection may be seen when the height change (i.e., Δz), which corresponds to horizontal segment Δx , is smaller than the length of the EM wavelength (i.e., λ). According to the thumb rule, the spacing between two x-values (Δx) should be less than equal to 0.1λ. Thus, the RMS height of the discrete one-dimensional case is

$$s = [\frac{1}{N-1} (\sum_{i=1}^{N} z_i^2 - N\bar{z}^2)]^{\frac{1}{2}} \tag{2.6}$$

Where N represent number of samples

$$\bar{z} = \frac{1}{N}\sum_{i=1}^{N} z_i \tag{2.7}$$

✓Surface correlation length

For the discrete one-dimensional situation, the correlation function ($\rho(\zeta)$) of the continuous random surface is mathematically defined as

$$\rho(\zeta) = \frac{\sum_{i=1}^{N+1-j} z_i z_{j+i-1}}{\sum_{i=1}^{N} z_i^2} \tag{2.8}$$

Where, $\zeta = (j-1)\Delta x$ and $j \geq 1$ is also an integer value. The correlation length is defined as the value of ζ at which $\rho(\zeta)$ becomes e^{-1}

✓RMS slope

The expression of RMS slope is defined in term of second derivative of the correlateion function at $\zeta = 0(i.e., \rho''(0))$

$$m = [-s^2\rho''(0)]^{\frac{1}{2}} \tag{2.9}$$

The value of RMS slope for the Gaussian correlation fucntion (i.e., $\rho(\zeta) = e^{\frac{-\zeta^2}{l^2}}$) is gives as

$$m = \sqrt{2}\frac{s}{l} \tag{2.10}$$

✓Volumteric soil moisture

The m_v observations were taken using Hydra Probe time-domain reflectometry sensor from a depth of 0-5 cm.

The significant difference between the water dielectric constant (about 80) and that of dry soil (approximately around 2-3) implies that the soil moisture content is correlated with its dielectric constant. Changes in the dielectric constant are detected by microwave sensors, which then offer information about the soil moisture content [46, 47]. Microwave remote sensing for determining surface soil moisture is based on this fundamental principle. The dielectric characteristics of soil moisture in the microwave areas have been the subject of numerous studies over the past four decades [47–51].

2.2.2 Smooth-surface criteria

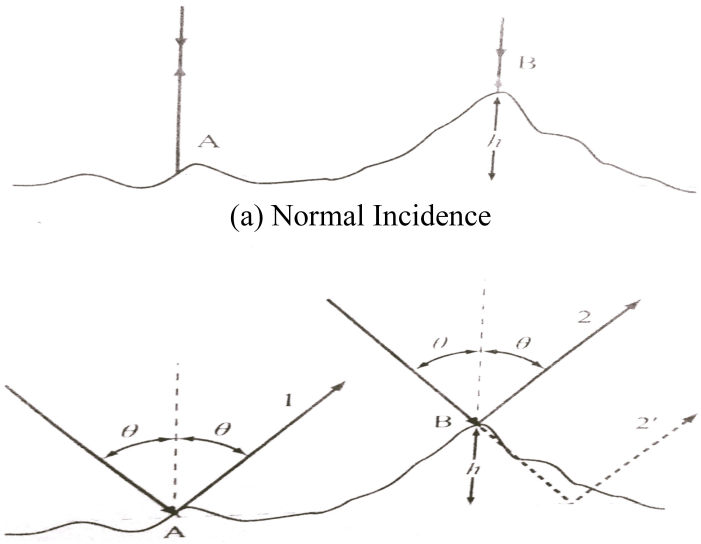

(a) Normal Incidence

(b) Oblique Incidence

Fig. 2.2 (a) Normal incidence and (b) Oblique incidence

Source:[3]

The electric fields of a ray that ordinarily strikes a flat surface and is subsequently reflected would have always been in phase. Nonetheless, if the surface is rough, as depicted in Figure 2.2, due to the higher surface at point B compared to point A, the electric field of a ray reflected from point B travels a 2h-distance shorter path. Consequently, the associated

phase difference is

$$\Delta\phi = 2kh = \frac{4\pi h}{\lambda};\ \ Wavevector(k) = \frac{2\pi}{\lambda} \tag{2.11}$$

However, for oblique incidence at an angle θ, as shown in Figure, the associated phase difference is

$$\Delta\phi = 2khcos\theta = \frac{4\pi h}{\lambda}cos\theta \tag{2.12}$$

There are two primary electromagnetic criteria that characterize the condition of surface roughness: the Rayleigh and Fraunhofer criteria. According to the Rayleigh roughness criterion, surfaces are considered smooth if $\Delta\phi < \frac{\pi}{2}$, which leads to the criteria

$$h < \frac{\lambda}{8cos\theta} \tag{2.13}$$

For random surfaces of RMS height of s, h may be substituted by s. Thus, the Equation 2.13 can be rewritten as

$$s < \frac{\lambda}{8cos\theta} \quad or \quad ks < 0.8(at\,\theta = 0) \tag{2.14}$$

The Rayleigh criterion can be helpful as a first-order classifier of surface roughness or smoothness. However, a more stringent criterion is required to model the scattering and emission behavior of natural surfaces in the microwave region, where the wavelength (λ) is usually of the order of the RMS height (s). To achieve this, we employ the criterion used to determine the far-field distance of an antenna, which stipulates that the maximum phase difference between the electric fields of the ray emanating from the center and edge of the antenna must be smaller than $\pi/8$ radians. This criterion is referred to as the Fraunhofer

roughness criterion, which relates to

$$s < \frac{\lambda}{32cos\theta} \quad or \quad ks < 0.2 \ (at\theta = 0) \tag{2.15}$$

2.2.3 Surface-scattering model

In the 1950s, several efforts were made to create mathematical models for randomly rough surfaces, resulting in the development of two approximative models. Rice developed the first approximate model in 1951 [52], known as the small perturbation model (SPM). In this model, the RMS height and correlation length are smaller than the incident electric field wavelength; hence, the model applies to slightly rough surfaces. The validity condition for the SPM is $ks < 0.3; kl < 3$; and $s/l < 0.3$.

Beckman and Spizzichino, in 1963 [53], developed the second approximate model known as the Kirchhoffs scattering model. This scattering model depicts EM scattering by surfaces with smooth fluctuations that have large average horizontal dimensions compared to λ. The Kirchhoffs scattering model used two types of approximations: the geometrical optics (GO) model and the physical optics(PO) model. For the GO and PO models, the total scattered field scattered by the undulating surface follows the validity requirements $kl > 6$ and $kl < 6$, respectively [54]. The Kirchhoffs scattering model includes an additional constraint associated with the surface RMS slope and average radius of curvature. For $kl > 6$, the surface radius of curvature is substantially larger than a wavelength, the scattering process is dominated by reflection. The correlation functions can be approximated by the first two elements of the Taylor expansion in the average scattered field. This led to the GO model. In contrast, for $kl < 6$ and $R_c > \lambda$ (i.e., the surface roughness radius of curvature is still substantially larger than a wavelength), then locally, both the reflection and diffraction are important in the scattering process. In this instance, the correlation function cannot be approximated, and the resultant model is referred to as the PO model.

Natural surfaces comprise a broad range of roughness scales over the microwave bands, which span a wavelength range from $1mm$ ($f = 300GHz$) to $30cm$ ($f = 1GHz$). Thus, the development scattering models from the 1960s are dedicated to a part of the roughness scale of relevance. The following three decades, numerous efforts were made to enhance the models and broaden their region of applicability, resulting in the development of an Integral Equation Model (IEM) [55] capable of addressing gaps between its predecessors. However, the model applicability is limited for backscatter configuration. Fung and his colleagues expanded the IEM's applicability to bistatic scattering during the next decade. The improved IEM scattering model, or I2EM, is the name given to the new model [56].

In the past four decades, numerous theoretical, empirical, semi-empirical, and bidirectional reflectance distribution function (BRDF) models have been constructed to mimic backscattering radar returns since the start of the SAR studies by correlating the backscatter coefficient with soil moisture and, more precisely, with the dielectric constants of bare soil and water [25, 37, 38, 51, 55, 57–68]. The theoretical model such as SPM, GO, PO, IEM, and I2EM are commonly used to build based on the wave theory of electromagnetic radiation. However, the applicability of these models is restricted to specific wavelength areas and surface roughness factors. Bindlish and Barros (2000) [69] used multi-frequency and multi-polarization data from the Spaceborne Imaging Radar C/X band Synthetic Aperture Radar (SIR-C/X-SAR) to estimate soil moisture content using the IEM inversion algorithm. Satalino et al. (2002) [70] found that ERS-1 and ERS-2 could not accurately extract two soil moisture classifications across flat, barren areas. By inverting the IEM theoretical model with adequately trained and regularized neural networks, we could estimate soil moisture with an overall root mean square error (RMSE) of $\Delta m_v = \pm 6\%$. The overall behavior of the backscattering coefficient can be predicted using theoretical models by altering the soil's surface roughness and moisture content [71]. However, their usefulness is

restricted due to the complicated and stringent necessity for parameterizing the vegetation and soil surface layer. This lead to difficulty in soil moisture retrieval [72].

Semi-empirical models are based on theoretical models with experimentally-derived parameters. Oh (1992) [37] created the first semi-empirical model based on scatterometer results for bare soil surfaces at varying roughness conditions for polarimetric radar soil moisture retrieval. The results showed that the cross-polarized ratio ($\frac{\sigma^0_{HV}}{\sigma^0_{VV}}$) is strongly dependent on *ks* and relatively less sensitive to soil moisture content. In Dubois (1995)'s semi-empirical technique, co-polarization backscattering coefficients σ^0_{HH} and σ^0_{VV} are given as nonlinear functions of surface dielectric constant, incidence angle, wavelength, and RMS surface roughness height(s) [38]. Backscattering models don't have site-specific issues like empirical models [73]. These models work best on bare Earth, not vegetation.

On the other hand, the empirical models generally use the experimental backscattering observation as a tool to build effective and efficient relations between backscattering coefficients with soil parameters and radar wave parameters of interest [73]. The validation zones of the theoretical backscattering models do not encompass a significant number of natural surfaces. Nevertheless, even when they do, the available backscattering models do not produce conclusions that are in good accord with experimental facts [37, 73]. In this instance, empirical backscattering models become significantly more important compared to their theoretical counterparts. The dependencies of the horizontal and vertical polarization-based empirical models were also developed to estimate soil surface parameters [74]. Although empirical methods can provide relatively accurate soil moisture results, they may not apply to datasets outside of the field observations. This is because a large number of experimental measurements are required to develop general statistical relations and establish an appropriate empirical model for the inversion of soil moisture from surface backscattering coefficients.

The natural soil surfaces are generally non-Lambertian and exhibit the anisotropic scattering effect, which depends on the structural properties of the surface. Generally, the reflected radiance depends on the transmitting zenith angle, the receiving zenith angle, and the difference between the transmitting and receiving azimuth angles [75–78]. The bi-directional reflectance distribution function (BRDF) describes this anisotropic effect by connecting incident irradiance to reflected radiance [79]. The BRDF is a fundamental property that describes a surface's reflectance, and it has received increasing attention in remote sensing. Moreover, the ground bi-directional reflectance data is becoming increasingly significant [80], particularly with the availability of multiangular remote sensing data from space-borne sensors, such as Multi-angle Imaging SpectroRadiometer (MISR), Moderate Resolution Imaging Spectroradiometer (MODIS), and various Polarization Analogue and Digital sensors (PAD). It is required to include the target's BRDF to calibrate reflectance into the reflectance at nadir, which normalizes reflectance and allows the comparison of data obtained from different angles [81, 82]. BRDF is one of the essential variables in using satellite data and deriving land bio-geophysical parameters of the Earth's surface [83, 84].

2.3 A review on vegetation observations and the volume scattering model

2.3.1 Vegetation observations

There are four essential vegetation parameters that are utilized to characterize the vegetation scattering model. These parameters are as follows:

✓**Leaf Area Index (LAI)**

Leaf Area Index (LAI) is defined as the ratio of one sided leaf area to the ground surface area. Its unit is given by m^2m^{-2} . The vegetation LAI at different phenological stages are measured using LAI-2200C plant canopy analyzer (LI-COR, Inc.)

✓**Fresh biomass (FBm) and Plant/Vegetation water content (PWC or VWC)**

The destructive sampling method was used to calculate the FBm and VWC/PWC of the vegetation. In this procedure, FBm were determined by multiplying the average weight of five samples of fresh vegetation by the vegetation density, which is the number of vegetation clusters per square meter. For the calculation of VWC, the average dry weight of the same five paddy clusters was determined by drying them in an oven at 60°C for 72 hours for the calculation of VWC. The value vegetations FBm and VWC were computed using Equations 2.16 and 2.17.

$$FBm = (\frac{1}{5}\sum_{i=0}^{5} W_{Fresh\ cluster_i})\eta \tag{2.16}$$

$$VWC = [\frac{1}{5}\sum_{i=0}^{5} (W_{Fresh\ cluster_i} - W_{Dry\ cluster_i})]\eta \tag{2.17}$$

Where $W_{Fresh\ cluster}$ is the weight of fresh vegetation, $W_{Dry\ cluster}$ is the weight of dry vegetation, η is vegetation density per square meter and n is the total number of vegattion sample.

✓**Plant height (d)**

A linear wooden scale of 1.5 meter long was used to measure the vegetation plant height under investigation.

2.3.2 Volume scattering model

The study of wave propagation and scattering in a random medium without boundaries or with plane boundaries in the field of volume scattering-based application has been thoroughly investigated by Ishimaru [85]. This review focuses on some of the volume

scatter approaches that have already been implemented in the creation of scattering models for radar returns from bounded random media. Volume scattering theories are typically used to build vegetation, snow, and sea ice scatter models. These theories are divided into two types: (1) The field approach and (2) The intensity approach. The field approach is further divided into three methods; (1) the Born approximation method, (2) the distorted Born approximation method, and (3) the Renormalization method. In the field approach, the average (or coherent) and scattered fields are first determined using the governing wave equations. The scattering coefficient is then derived using the average scattered power. The wave equation is frequently solved iteratively. Stogryn, in 1974 [86], and Tsang and Kong, in 1978 [87], showed that there is no depolarized backscattering in the first-order result. However, second-order results give depolarized backscattered power, but the radar return must be modest (lower in field amplitude and power). No report has shown that the second-order term can explain cross-polarized terrain returns. Furthermore, the intensity approach includes two methods; (1) the Radiative transfer method and (2) the Matrix doubling method. However, our interest is in the radiative transfer method. Thus, subsections solely discuss only the radiative transfer concept.

✓Radiative transfer model/method (RTM)

Numerous researchers have investigated the relationship between radiative transfer theory and Maxwell's equations [85, 88–93]. Collett, in 1977 [91] showed that the radiative transfer theory specific intensity and the electromagnetic field mutual-coherence function form an accurate Fourier transform pair for statistically homogenous fields in a vacuum. In 1981, Fante demonstrated that a certain intensity might be defined in a lossless dielectric medium consistent with Maxwell's equations if the field correlation tensor and relative permittivity function meet specific requirements [93]. Zuniga and Kong [89] constructed modified radiative transfer equations (RTE) from the Bethe-Salpeter equation with the ladder approximation and the Dyson equation with the nonlinear approximation. The

added factor in modified RTE corrects conventional RTE's for transverse electric and transverse magnetic phase velocity differences. Although the stringent criteria for the validity of the standard radiative transfer equations are not entirely known, a couple of fundamental qualities need to be present in a situation to make it possible to put this method into practice. First, the scattered field needs to be designed to eliminate the significance of cross-correlation terms. Second, the interaction between scatterers in the far zone is the only one that matters.

The First-order multiple scattering studies have made considerable use of the radiative transfer method for homogeneous media containing scatterers with known scattering phase matrices [85, 94–101]. The transfer equations can be stated using an upward internsity ($I^+(\theta,\phi,z)$) and a downward intensity ($I^-((\pi-\theta,\phi,z)$) vector, as follows

$$cos\theta\frac{dI^+}{dz}(\theta,\phi,z) = -k_e(\theta,\phi)I^+(\theta,\phi,z) + \int_0^{\frac{\pi}{2}} sin\theta' d\theta' \left[\int_0^{2\pi} d\phi' P(\theta,\phi;\theta',\phi')I^+(\theta',\phi',z) + \int_0^{2\pi} d\phi' P(\theta,\phi;\pi-\theta',\phi')I^-(\pi-\theta',\phi',z)\right] \tag{2.18}$$

$$-cos\theta\frac{dI^-}{dz}(\pi-\theta,\phi,z) = -k_e(\pi-\theta,\phi)I^-(\pi-\theta,\phi,z) + \int_0^{\frac{\pi}{2}} sin\theta' d\theta' \left[\int_0^{2\pi} d\phi' P(\pi-\theta,\phi;\theta',\phi')I^+(\theta',\phi',z) + \int_0^{2\pi} d\phi' P(\pi-\theta,\phi;\pi-\theta',\phi')I^-(\pi-\theta',\phi',z)\right] \tag{2.19}$$

Where, P and k_e are 4×4 phase and extinction coefficient matrix and derived by lshirnaru and Cheung in 1980 [102]. For the spherical volume scatterer, the phase matrix becomes diagonal. For spherical volume scatterers, it is convenient to compute vegetation optical depth using Equation 2.20

$$\tau = \int_z^0 \frac{k_a}{1-w} dz \tag{2.20}$$

Where k_a and w are absorption coefficient and scattering albedo, respectively. The fourier series expansions can be applied to both the intensity and phase functions in the scattering problem concerning azimuth angle, followed by the azimuthal integration. First-order linear differential equations can be generated for each Fourier component by applying the quadrature approach to an Θ' integral [94]. The usual eigenvalue-eigenvector approach can be used to solve this set of equations or the finite difference method can be used to convert the differential equations to algebraic equations further and then solve the set by the standard matrix approach [103].

The simplicity of this technique's conceptual foundation is its primary advantage. To preserve a decent level of stability during matrix inversion, the number of quadrature points employed is restricted to 16 or fewer. As the layer approaches a half-space, the rank of the matrix must be decreased in order to eliminate the intensities reflected from the lower layer. This is manageable through singular-value decomposition [104]. However, the limited number of quadrature points necessitates the employment of slowly varying, well-behaved phase matrices whose angular variations lack abrupt peaks. This obstacle has not been conquered. The phase coherence effect is neglected in multiple scattering computations, which is a well-known shortcoming of all formulations of radiative transfer. However, the transfer formulation is the easiest and most efficient technique to manage multiple scattering at this moment.

2.4 Scatteromters

During the early stages of SAR research, the scatterometer at ground level was utilized extensively to understand better the scattering behavior of different targets to various SAR configurations. It let scientists develop and try out new methods before SAR satellite systems were built and before data from space was available. Scatterometers can also

be utilized in unique ways to investigate microwave interaction phenomena with Earth features that are difficult to examine using airborne and space-borne technologies.

In 1985, the Canada Centre for Remote Sensing (CCRS) designed a ground-based scatterometer for agricultural studies. A hydraulic boom is mounted on the flatbed truck, supporting a three-band arrangement. The scatterometer collected L, C, and Ku bands (1.5, 5.2, and 12.8 GHz) data at HH, VV, HV, and VH polarizations. The boom's incident angle ranged from 20° to 50°. The CCRS scatterometer was used to investigate crop classification performance in the early stages of its development. The wheat crop's daily impacts on backscattering coefficients at Ku, C, and L band were explored by Brisco [105]. The variation in the daily backscattering coefficient due to increased crop geometry was found different at the highest frequency compared to the lower frequency. Backscattering coefficients were sensitive to the day-to-day changes in the amount of water in the crop canopy till the wheat crop growth stages. However, after the maturity stage, backscattering coefficients were sensitive to the amount of water in the soil. For crop separability information, a multi-temporal ground-based Ku, C, and L band scatterometer dataset of spring wheat (bearded and non-bearded), barley, canola, and summer/allow crop types were analyzed by Brisco [106]. In addition, F-ratios were calculated and ranked to assess the impact of frequency, polarization, and incidence angle on class separability. The Scatterometer data are effective for estimating soil moisture using three surface roughness-based models [37, 38, 55]. The performance of these models was analyzed for harrow and seed plots. McNairn, in 1996 [107] assessed models to predict soil moisture and surface roughness using a dual incidence angle approach.

NASA's SMAP algorithmic development prompted numerous ground-based scatterometer investigations [108]. NASA's combined radar/radiometer (ComRAD) equipment is a dual-polarized SMAP simulator mounted on a truck equipped with a radiometer and scatterometer. The instrument was installed on a 19-m hydraulic platform and equipped

to measure at a 40° incidence angle identical to SMAP, and it can measure in both incidence and azimuth angles. Initial investigations focused on studying microwave extinction within the forest medium to retrieve soil moisture information [109]. O'Neill in 2013 acquired passive and active L band measurements for soybean and corn crops to optimize SMAP retrieval methods [110]. These data showed the impact of change vegetation in biophysical parameters on the measurements and the correlation between active and passive observations.

The fully polarimetric ground-based University of Florida L band Automated Radar System (UF-LARS) measures backscattering at intervals of 10-15 minutes [111]. Typically, measurements were taken from a height of around 25 meters above the ground at an incidence angle of 40 degrees. The UF-LARS's temporal variation of backscattering radar returns from vegetation and upper layer of the land surface (0-5 cm) soil moisture fluctuations provides insights into microwave interaction with land bio-geophysical parameters. The vegetation density and meaningful data also facilitate the development and validation of radiative transfer models for information retrieval. The UF-LARS has been used to evaluate the sensitivity of backscattering to volumetric soil moisture [112] and vegetation growth parameters [111], the benefit of combining active and passive microwave observations for soil moisture estimation [113], and uncertainty in the SMAP downscaling algorithm for sweet corn [112]. Monsivais-Huertero, in 2015 examined bias correction methods used to estimate soil moisture from active UF-LARS and passive University of Florida L band Microwave Radiometer (UF-LMR) data [114].

2.5 State-of-the-art

In recent decades, the backscattered electromagnetic fields from the Earth's topographical and morphological features, such as vegetation lands and bare lands, etc., have been studied using scatterometers at the ground, aircraft, and space-borne altitudes. However,

bistatic electromagnetic scattering from vegetated fields and random rough bare lands has received less attention since its application is not as straightforward as backscattering. Numerous theoretical advancements have been made for bistatic scattering from vegetated and bare lands, but they have not been extensively employed and evaluated using bistatic measurement [115–119]. Consequently, the utility and reliability of bistatic scattering are mainly unknown. Therefore, a comprehensive examination of the bistatic observable quantities is required to provide valuable insights for land surface applications. In addition, experimental investigation of bistatic scattering is useful for predicting the performance of antennas operating in the presence of the ground and optimizing radar parameters for monitoring land bio-geophysical parameters [53, 120]. Moreover, recent developments in topography modeling for radar bistatic scattering from volume scatterer overlaying rough lands have significant potential to yield scatterer parameter information compared to the backscattering case.

This thesis investigates the nature of polarimetric bistatic specular scattering from vegetation using an indigenous designed bistatic scatterometer system. The investigation is carried out over a wide specular incidence angular range from 20° to 60° at X, C, and L bands. While numerous theoretical approaches to vegetation scattering have been established, a first-order radiative transfer model was used to analyze vegetation scattering comprehensively. Due to the validity domains of the measured soil surface parameters, only the sensitivity of Kirchhoff's model to soil moisture and surface roughness has been examined. The simulation results were compared to the bistatic scattering response measured from the bistatic scatterometer system to assess the scattering model's integrity. The inverse formulation of the developed scattering model is used to retrieve land bio-geophysical parameters information. Furthermore, machine learning techniques, notably Support Vector Regression (SVR) with linear, polynomial, and radial kernels, were utilized

to construct a model that was independent of system and target characteristics and could be inverted for estimation of land bio-geophysical parameters.

****